Electrolyte-gated-organic field effect transistors functionalized by lipid monolayers with tunable pH sensitivity for sensor applications

Tin Phan Nguy, Ryoma Hayakawa, Volkan Kilinc, Matthieu Petit, Yemineni S L V Narayana, Masayoshi Higuchi, Jean-Manuel Raimundo, Anne Charrier, Yutaka Wakayama

Template for APEX (Jan. 2014)

Electrolyte gated-organic field effect transistors functionalized by lipid monolayers with tunable pH sensitivity for sensor applications

Tin Phan Nguy[1,2], Ryoma Hayakawa[1], Volkan Kilinc[3], Matthieu Petit[3], Yemineni S L V Narayana[4], Masayoshi Higuchi[4], Jean-Manuel Raimundo[3], Anne Charrier[3], and Yutaka Wakayama[1,2*]

[1]*International Center for Materials Nanoarchitectonics (WPI-MANA), National Institute for Materials Science (NIMS), 1-1 Namiki, Tsukuba 305-0044, Japan.*
[2]*Department of Chemistry and Biochemistry, Faculty of Engineering, Kyushu University, 1-1 Namiki, Tsukuba 305-0044, Japan.*
[3]*Aix-Marseille Univ, CNRS, CINaM, Marseille, France.*
[4]*Research Center for Functional Materials, National Institute for Materials Science (NIMS), 1-1 Namiki, Tsukuba 305-0044, Japan.*

E-mail: WAKAYAMA.Yutaka@nims.go.jp

Abstract: Electrolyte-gated organic field effect transistors (EG-OFETs) functionalized by engineered lipid monolayers (LMLs) are investigated to tune pH sensitivity for sensor application. The EG-OFET functionalized by OH-terminated LML shows linear dependence on the physiological pH range (4-8). Meanwhile, the LML with polar-head groups presents limited pH sensitivity only in a certain pH range. In contrast, the methyltrichlorosilane (MTS) passivation of the LML head-group makes the EG-OFET non sensitive in a broad pH range (1.68-12). These findings suggest that our proposed transistors have the potential to construct versatile sensor applications with the controllable pH sensitivity.

In recent years, organic field effect transistors (OFETs) have been widely utilized for sensor applications.[1–4] OFETs provide versatile platforms to achieve high selectivity and sensitivity even with small input signals.[5–9] With respect to sensor applications in the aqueous environment, liquid electrolytes have been widely used as electrical gates in these transistors.[10–15] Then, metallic gate electrode is immersed into the electrolyte solution. Of importance is that the electrolyte-gated OFETs (EG-OFETs) effectively work at the millivolt range. This is owing to the high capacitance (1-20 μFcm^{-2})[16,17] of an electrical double layer (EDL) formed at the interface between the electrolyte solution and organic semiconductor channel. This merit leads to an ultra-low threshold voltage (V_{th}) under 1 V, which is effective to avoid any electrochemical reaction in the electrolyte solution.[17,18] Here, it should be noted that V_{th} is highly responsive to surface charges provided from analytes such as ions or biomolecules.[8,12,19] Therefore, the ultra-low V_{th} is advantageous to detect even small signals.

Because of these features, the EG-OFETs are suitable for sensing ions and biomolecules in the aqueous environment. However, the EG-OFET-based sensors faced following obstacles. First, the detection of these analytes is typically carried out in the presence of interfering ions, e.g., potassium and sodium. These ions are well known to degrade the transistor performance because they act as electrical dopants for OFETs.[16,17,19] The stable operation of EG-OFETs in such aqueous environment, therefore, still remains as a challenge.[17,20–22] Second, specific sensing probes should be attached on the surface of the transistor channels for detecting analytes such as ions and proteins.

To satisfy these requirements, we investigated the EG-OFETs with engineered lipid membranes. The ultrathin lipid monolayers (LMLs) with the thickness of 2.2 nm[23] were formed on the poly(3-hexylthiophene-2,5-diyl) (P3HT) films, which were employed as semiconductor channels due to its stability in the aqueous environment.[10,15] The first striking point is that the LMLs was proved to protect the transistor channels from direct exposure to the electrolyte solution. That is, LML enabled the stable transistor operation even in aqueous conditions by reducing electrochemical doping into the transistor channels. Second, the LMLs were functionalized by attaching head groups to provide capability for tuning pH sensitivity. Then, stability, repeatability and sensitivity to pH levels of the EG-OFETs were examined by changing head-groups of the LMLs. Importantly, we found that the transistors with OH-terminated LMLs demonstrated a linear sensitivity with pH level in the range of 4 to 12. Meanwhile, methyltrichlorosilane (MTS)-terminated LMLs showed no sensitivity against pH levels and significantly stable operation even with the

presence of high ion concentration in the electrolyte solution. In this manner, our EG-OFETs with engineered LMLs provide an innovative concept for further biosensors or chemical sensors.

Figure 1 (a) shows the structure of the EG-OFET, molecular structure of P3HT and those of LMLs. Of importance is that the LMLs have distinct head groups. The first LML consists of phosphocholine (DCPC) lipids. This lipid has a zwitterion with a large permanent dipole moment induced by a negative charge of phosphate (PO_4^-) and a positive charge of trimethylamine ($N^+(CH_3)_3$) at the head group. The second one is DC-glycerol (DCOH) lipid monolayer, which has the neutrally charged OH-functional groups. Then, the OH-functional groups can be further functionalized by MTS groups to form the third LML (DC-MTS).

The top-gate and the bottom-contact-type EG-OFETs were prepared on 200-nm-thick SiO_2/p-Si substrates, where P3HT films were used as the transistor channel. First, source and drain electrodes were patterned on SiO_2/p-Si substrates through a shadow mask by thermal evaporation. P3HT powder (Sigma Aldrich) was dissolved in chlorobenzene solvent, followed by heating the solution at 60 ºC for 30 minutes to obtain 0.75 wt% solution. After passing through a filter with a pore size of 200 nm, P3HT solutions were spin-coated on the substrates with patterned electrodes. The P3HT films thus prepared were annealed at 150 ºC in a vacuum to eliminate the residual solvent. Finally, a PDMS (polydimethylsiloxane) container was carefully sealed on top of the P3HT film. The gate bias voltage was applied by the immersion of an Au gate electrode in electrolyte solution.

Lipid molecules formed a monolayer on the P3HT film by following protocol.[15,23,24] 1,2-bis(10,12-tricosadiynoyl)-sn-glycero-3-phosphocholine phospholipid (DCPC) in the form of powder was purchased from Avanti Polar Lipids (AL, USA) and used as received. DC-glycerol (DCOH) lipids were synthesized from DCPC lipid (Fig. S1).[8,23,25] A LML of DC-glycerol was formed on the P3HT film based on the hydrophobic interaction between alkyl chains of the DCOH lipid and P3HT film. The polymerization at the middle of lipid molecules (Fig. S2) improved the mechanical and electrical stability of LML.[23,24] Then, DC-MTS were obtained by exposing the device to the MTS solution diluted by 1,4-dioxane (Sigma-Aldrich). The more detailed conditions were described in the supporting information.[8,23] Consequently, the ultrathin (2.2 nm) phospholipid monolayer sustainably covered the P3HT surface. The attenuated total reflection Fourier transform infrared (ATR-FTIR) measurement confirmed the formation of the LML on P3HT film.[24] The surface morphology of pristine P3HT and lipid on P3HT were examined by AFM (SII,

SPI4000). AFM images showed the flat P3HT film surface without (Fig. 1(b)) and with (Fig. 1(c)) the DCPC. The surface roughness (RMS) values were 0.56 nm and 0.92 nm, respectively. P3HT films with DCOH and DC-MTS also showed similar results with RMS values of 0.85 nm and 0.77 nm, respectively, proving that the uniform formation of the LMLs on the P3HT film.

First of all, we investigated fundamental properties of three kinds of EG-OFETs: the pristine P3HT without LMLs and the P3HT with respective LMLs (DCPC and DCOH). The I-V curves were measured by using a semiconductor parameter analyzer (Agilent B1500A) under ambient conditions. The phosphate-buffered solution with a fixed pH of 6.86 was used as an electrolyte gate to evaluate the performance of EG-OFET. Figure 2 shows the drain current (I_{DS})-gate voltage (V_{GS}) curves of three devices, where the gate voltage was swept from +0.4 V to −0.5 V at a fixed drain voltage of – 0.5 V. The saturation region was clearly observed in a typical output curve of EG-OFET in Fig. S3. The V_{th} was calculated with the following equations.[26)]

$$I_{DS} = \frac{W}{2L}\mu C_i(V_{GS} - V_{th})^2 \quad (1)$$

where W (100 μm), L (2000 μm), μ and C_i are the width and length of the transistor channel, carrier mobility and the capacitance of the gate dielectric layer, respectively. The V_{th} of the pristine P3HT transistor was estimated to be + 70 mV (±27 mV). Meanwhile, those of the transistors with DCOH and DCPC LMLs were −29 mV (±33 mV) and +24 mV (±34 mV), respectively. In this manner, three devices showed the ultralow threshold voltage (V_{th}), even though there were slight differences in the V_{th} values. Additionally, the estimated carrier mobilities of pristine P3HT and P3HT with DCOH lipid were same order, 7.2×10^{-3} $cm^2V^{-1}s^{-1}$ and 4.3×10^{-3} $cm^2V^{-1}s^{-1}$, respectively. The mobilities are comparable to those reported in the P3HT-based EG-OFETs,[10,17)] suggesting that the LMLs had moderate impact on the carrier transport in the channel layers.

Clear differences were observed in the forwards and backwards potential sweeps. The pristine P3HT showed a hysteresis around low gate bias range of +0.4 to 0 V (Fig. 2(a)). In contrast, the EG-OFETs covered by the LMLs demonstrated negligible hysteresis in the loops as can be seen in Figs. 2(b) and (c). The observed hysteresis in the pristine P3HT can be ascribed to the ion doping from the electrolyte solution into the P3HT channel during the potential sweeps. Meanwhile, the LMLs suppressed such electrochemical doping effect. This advantage of the LML was pronounced in the long-term operation as described below.

The long-term operation stability in the electrolyte solution is strictly required for sensor applications. The operation stability of three devices was evaluated by repeating measurements ten cycles for 2 hours in electrolyte solution. We observed the gradual decrease in V_{th} with significant deviation in the pristine P3HT EG-OFET as shown in Fig. 2(d). This result can be explained by the doping from electrolyte solution into the P3HT channel. In contrast, both LMLs on the P3HT films improved the stability of the EG-OFET for long-term measurement; no shifts in V_{th} were observed as shown in Figs. 2(e) and 2(f)). The deviations at each cycle were also negligibly small. These results also indicate that the LML is effective to reduce the ion doping into the P3HT channel. This is a clear advantage for the sustainable operation of EG-OFETs in electrolyte solution.

For sensor application, including specific ion and biological sensors, the control of pH sensitivity is a key factor. Therefore, we discussed how to design the head groups of LMLs for tuning pH sensitivity. The pH sensitivities of EG-OFETs with two kinds of LMLs, DCOH and DCPC, were compared to examine the capability of EG-OFETs with LMLs as pH sensors. Then, the pristine EG-OFET with a non-functionalized P3HT channel was evaluated as a reference. The standard pH solutions in a range from 1.68 to 12 were used to examine the pH sensitivity of devices. The variation in the V_{th} (ΔV_{th}) depending on the pH level was measured for respective EG-OFETs. The transfer curves were recorded in the V_{GS} range of 0 to −300 mV at fixed V_{DS} of −300 mV. The low range of V_{GS} was to avoid any electrolysis process caused by pH variation.[18] The obtained results showed significant differences in ΔV_{th} as shown in Figs. 3(a)-(c). The pristine EG-OFET showed no dependence of V_{th} on the pH level (Figure 3(a)). This was resulted by the non-pH sensitivity of alkyl chains of the P3HT film. However, the pristine EG-OFET presented significant deviations of V_{th}. The doping of electrolyte ions is the reason for the unstable operation of the pristine EG-OFET in pH (electrolyte) solution.

In a case of the DCPC LML, no clear dependence of ΔV_{th} was observed although it showed wide variations against pH levels as shown in Figure 3(b). This result was probably due to the intrinsic characteristics of zwitterionic head groups of DCPC lipid.[27–32] In pH range of 4 to 8.5, the DCPC lipid is electrically neutral due to the co-existence of both positive and negative charged groups.[28,29] As a result, the transistor with DCPC lipid showed only marginal ΔV_{th} in this pH range. Meanwhile, the V_{th} was dramatically shifted to positive side above pH level of 8. This is due to the neutralization of positively charged groups ($pKa_2 \approx 10$) while the negatively charged groups still remained.[31,33,34] The negative ΔV_{th} observed below pH of 4 was supposed to be induced by positively charged head

groups ($pKa_1 \approx 1.7$). In this manner, DCPC LML showed complicated variations in ΔV_{th} depending on the surface charges.

In contrast, the DCOH LML obviously showed linear dependence of ΔV_{th} on the pH level as shown in Figure 3(c). The ΔV_{th} was ranging from +50 mV to -100 mV in the range of pH from 4 to 12. The sensitivity is approximately 17.76 mV per pH. This result is explained by the interaction of H_3O^+ at OH group. This formation caused the variation in the charge density on the surface[35,36], modulating the capacitance of EDL[36]. As a result, the charge accumulation in the transistor channel was modulated. Hence, the transfer curves gradually shifted to negative gate voltage according to the pH level. This tendency is shown in Fig. S6. Additionally, the devices showed the chemically stability with small hysteresis when changing pH values from acid to and vice versa (Fig. S7). Under pH of 4, the ΔV_{th} showed the independence on the pH level. These results emphasize the importance of head groups of the LML. The chemical reactions of the head groups in different pH levels significantly affect on the performance of the EG-OFETs. Furthermore, the EG-OFET with the DCOH showed a linear sensitivity with the physiological pH range of 4-8, which is adaptable in biology and medicine applications.[37] This finding is useful to fulfill sensing applications with biological friendliness.

However, the development of sensors with non-sensitivity to pH variations is also crucial in some cases. This is because the sensors are required to selectively detect only the analytes (ions or proteins) even in electrolyte solution with different pH levels.[8] For these purposes, we modified the DCOH LML by silanization to convert the head group from OH to MTS (denoted as DC-MTS LML). Then, we evaluated the pH sensitivity and operation stability of the EG-OFET with DC-MTS LML. Details of the measurement conditions were same to those of other EG-OFETs. The low V_{th} (+120 mV) was confirmed. Importantly, the transistors became non-sensitive to the pH variation as shown in Fig. 4(a). No variation in V_{th} (ΔV_{th} =0 mV) was observed regardless of pH levels. The deviation of V_{th} at each pH level was also enough small due to the reduced doping effect into the P3HT film. The results indicate that the MTS groups successful passivated the OH-groups. Furthermore, the devices showed a stable operation even after exposing to the organic solvent (Fig. 4(b)). The V_{th} showed a negligible change even after repeated measurements for 2 hours. It should be emphasized that this technique provides the potential benefit for passivating OH terminals as well as for grafting other receptors onto the LML at R-positions in Fig. S2. That is, the EG-OFET with DCOH monolayer has high potential in further functionalization by specific probes for versatile sensor application.

In summary, we have developed novel EG-OFETs by functionalizing transistor channels with the engineered LMLs. The engineered LML contributed to improve EG-OFET operation by preventing the doping effect from electrolyte solution into the transistor channels. The ΔV_{th} was negligible small even after repeated operations in the electrolyte solution for a long time. The performance of EG-OFET was found to be controlled by the different functional groups of the LML. The EG-OFET with DCOH LML showed the pH sensitivity which satisfied the physiological pH range (4-8) as reported by G. K. Schwalfenberg et al.,.[37] On the contrary, the EG-OFET the DC-MTS LML showed the independence on pH level in a large range (1.68 to 12). This result implies that the EG-OFET with DCOH LML has a potential for further sensor development because specific receptors can be easily attached to LML for the detection of ions and protein molecules. Our approach will pave the way for development of new sensor applications in chemical and biological fields.

Acknowledgments

This research was performed under the framework of the Strategic International Collaborative Research Program (SICORP) supported by the Japan Science and Technology Agency (JST) and L'Agence Nationale de la Recherche (ANR), and was supported by the World Premier International Center (WPI) for Materials Nanoarchitectonics (MANA) of the National Institute for Materials Science (NIMS), Tsukuba.

References

1) R. Hayakawa, M. Petit, K. Higashiguchi, K. Matsuda, T. Chikyow, and Y. Wakayama, Org. Electron. Physics, Mater. Appl. **21**, 149 (2015).

2) S. Lai, M. Barbaro, and A. Bonfiglio, Sensors Actuators, B Chem. **233**, 314 (2016).

3) M. Yun, A. Sharma, C. Fuentes-Hernandez, D. K. Hwang, A. Dindar, S. Singh, S. Choi, and B. Kippelen, ACS Appl. Mater. Interfaces **6**, 1616 (2014).

4) B. Yaman, I. Terkesli, K. M. Turksoy, A. Sanyal, and S. Mutlu, Org. Electron. Physics, Mater. Appl. **15**, 646 (2014).

5) G. Horowitz, Adv. Mater. **10**, 365 (1998).

6) F. Werkmeister and B. Nickel, J. Mater. Chem. B **1**, 3830 (2013).

7) T. Minami, T. Sato, T. Minamiki, K. Fukuda, D. Kumaki, and S. Tokito, Biosens. Bioelectron. **74**, 45 (2015).

8) T. D. Nguyen, A. Labed, R. El Zein, S. Lavandier, F. Bedu, I. Ozerov, H. Dallaporta, J. M. Raimundo, and A. M. Charrier, Biosens. Bioelectron. **54**, 571 (2014).

9) L. Torsi, M. Magliulo, K. Manoli, and G. Palazzo, Chem. Soc. Rev. **42**, 8612 (2013).

10) L. Kergoat, L. Herlogsson, D. Braga, B. Piro, M. C. Pham, X. Crispin, M. Berggren, and G. Horowitz, Adv. Mater. **22**, 2565 (2010).

11) L. Kergoat, B. Piro, M. Berggren, M. C. Pham, A. Yassar, and G. Horowitz, Org. Electron. Physics, Mater. Appl. **13**, 1 (2012).

12) S. Lai, M. Demelas, G. Casula, P. Cosseddu, M. Barbaro, and A. Bonfiglio, Adv. Mater. **25**, 103 (2013).

13) M. Magliulo, A. Mallardi, M. Y. Mulla, S. Cotrone, B. R. Pistillo, P. Favia, I. Vikholm-Lundin, G. Palazzo, and L. Torsi, Adv. Mater. **25**, 2090 (2013).

14) F. Buth, A. Donner, M. Sachsenhauser, M. Stutzmann, and J. A. Garrido, Adv. Mater. **24**, 4511 (2012).

15) T. P. Nguy, R. Hayakawa, V. Kilinc, M. Petit, J.-M. Raimundo, A. Charrier, and Y.

Wakayama, Jpn. J. Appl. Phys. **58**, SDDH02 (2019).

16) F. Buth, D. Kumar, M. Stutzmann, and J. A. Garrido, Appl. Phys. Lett. **98**, 2009 (2011).

17) S. Cotrone, M. Ambrico, H. Toss, M. D. Angione, M. Magliulo, A. Mallardi, M. Berggren, G. Palazzo, G. Horowitz, T. Ligonzo, and L. Torsi, Org. Electron. Physics, Mater. Appl. **13**, 638 (2012).

18) K. Schmoltner, J. Kofler, A. Klug, and E. J. W. List-Kratochvil, Adv. Mater. **25**, 6895 (2013).

19) T. Minamiki, Y. Hashima, Y. Sasaki, and T. Minami, Chem. Commun. **54**, 6907 (2018).

20) O. Knopfmacher, M. L. Hammock, A. L. Appleton, G. Schwartz, J. Mei, T. Lei, J. Pei, and Z. Bao, Nat. Commun. **5**, 2954 (2014).

21) R. Porrazzo, S. Bellani, A. Luzio, E. Lanzarini, M. Caironi, and M. R. Antognazza, Org. Electron. Physics, Mater. Appl. **15**, 2126 (2014).

22) T. Cramer, A. Campana, F. Leonardi, S. Casalini, A. Kyndiah, M. Murgia, and F. Biscarini, J. Mater. Chem. B **1**, 3728 (2013).

23) A. Kenaan, R. El Zein, V. Kilinc, S. Lamant, J. M. Raimundo, and A. M. Charrier, Adv. Funct. Mater. **28**, 1801024 (2018).

24) A. Charrier, T. Mischki, and G. P. Lopinski, Langmuir **26**, 2538 (2010).

25) T. D. Nguyen, R. El Zein, J. M. Raimundo, H. Dallaporta, and A. M. Charrier, J. Mater. Chem. B **1**, 443 (2013).

26) H. Ishii, K. Kudo, T. Nakayama, and N. Ueno, *Electronic Processes in Organic Electronics: Bridging Nanostructure, Electronic States and Device Properties* (Oxford University Press, 2015).

27) K. Arand, D. Stock, M. Burghardt, and M. Riederer, J. Exp. Bot. **61**, 3865 (2010).

28) J. Stein, Biophys. J. **49**, (1986).

29) N. A. Alhakamy, I. Elandaloussi, S. Ghazvini, C. J. Berkland, and P. Dhar, Langmuir **31**, 4232 (2015).

30) A. D. Petelska and Z. A. Figaszewski, Biophys. J. **78**, 812 (2000).

31) S. Pullanchery, T. Yang, and P. S. Cremer, J. Phys. Chem. B **122**, 12260 (2018).

32) M. Mackiewicz, J. Romanski, and M. Karbarz, RSC Adv. **4**, 48905 (2014).

33) J. Kotyńska and Z. A. Figaszewski, Biochim. Biophys. Acta - Biomembr. **1720**, 22 (2005).

34) A. D. Petelska, J. R. Janica, J. Kotynska, U. Łebkowska, and Z. A. Figaszewski, J. Membr. Biol. **245**, 15 (2012).

35) I. Y. Sohn, D. J. Kim, J. H. Jung, O. J. Yoon, T. Nguyen Thanh, T. Tran Quang, and N. E. Lee, Biosens. Bioelectron. **45**, 70 (2013).

36) Y. Qin, H. J. Kwon, M. M. R. Howlader, and M. J. Deen, RSC Adv. **5**, 69086 (2015).

37) G. K. Schwalfenberg, J. Environ. Public Health **2012**, (2012).

Figure Captions

Fig. 1. (a) A schematic illustration of electrolyte gated-organic field transistor with three kinds of LMLs. The molecular structures of respective lipids, i) DCPC, ii) DCOH and iii) DC-MTS, are shown on the right side. The surface morphology of (b) pristine P3HT film and (c) DCPC lipid monolayer on the P3HT film. The AFM images showed the uniform of P3HT film before and after lipid monolayer deposition.

Fig. 2. Transfer curves of EG-OFETs with (a) pristine P3HT, (b) P3HT with DCPC layer and (c) P3HT with DCOH layer. The variations in V_{th} (ΔV_{th}) with repeated transistor measurements: (d) pristine P3HT (e) P3HT with DCPC LML (f) P3HT with DCOH LML.

Fig. 3. Variation in threshold voltage (ΔV_{th}) of EG-OFET in electrolyte solutions with different pH levels: (a) pristine P3HT (b) P3HT with DCPC lipid and (c) P3HT with DCOH lipid.

Fig. 4. (a) pH dependence of ΔV_{th}, showing no variations. (b) ΔV_{th} after repeated operations.

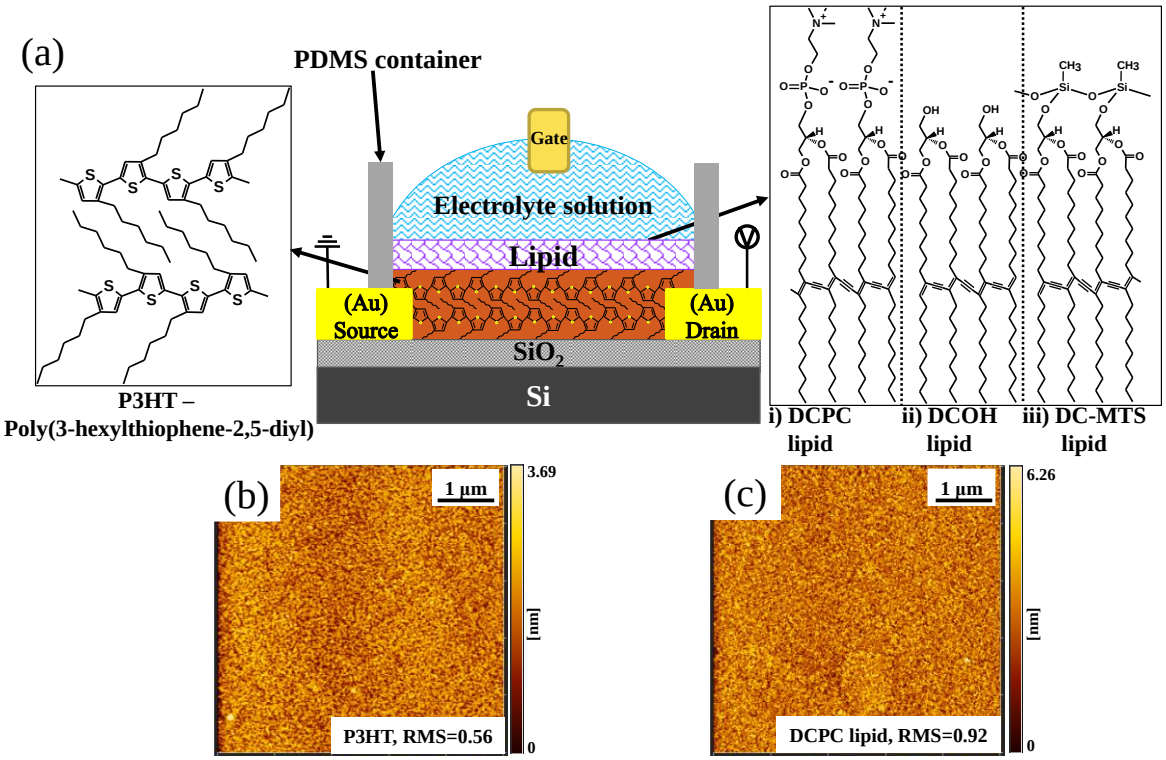
(a)
PDMS container
Gate
Electrolyte solution
Lipid
(Au) Source
(Au) Drain
SiO2
Si
P3HT – Poly(3-hexylthiophene-2,5-diyl)
i) DCPC lipid
ii) DCOH lipid
iii) DC-MTS lipid
(b)
1 µm
3.69
[nm]
0
P3HT, RMS=0.56
(c)
1 µm
6.26
[nm]
0
DCPC lipid, RMS=0.92

Fig.1.

Template for APEX (Jan. 2014)

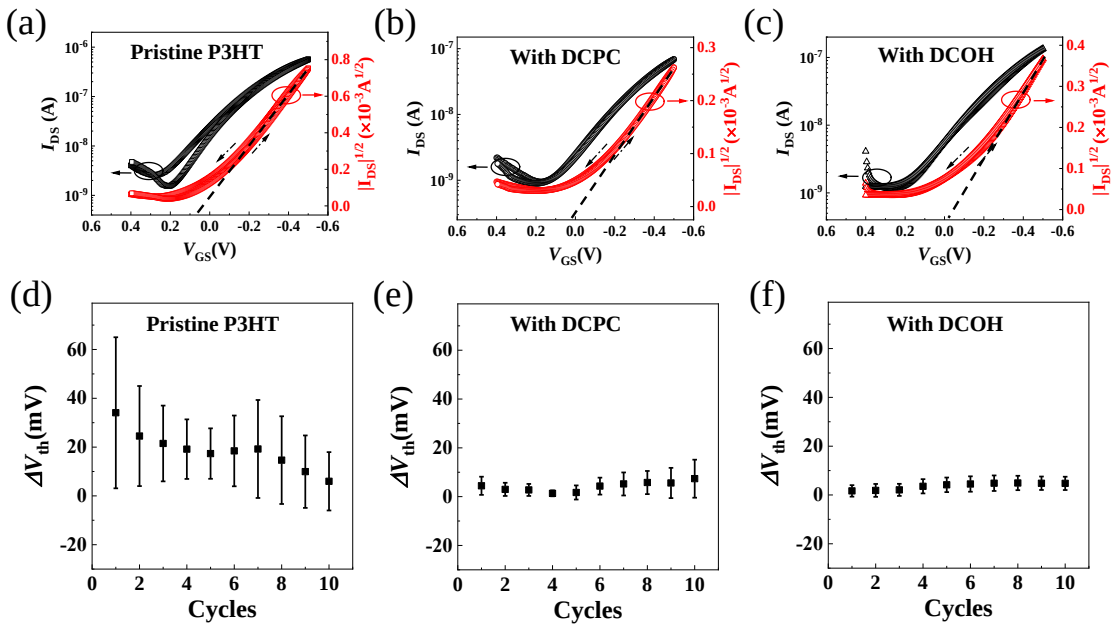

Fig. 2.

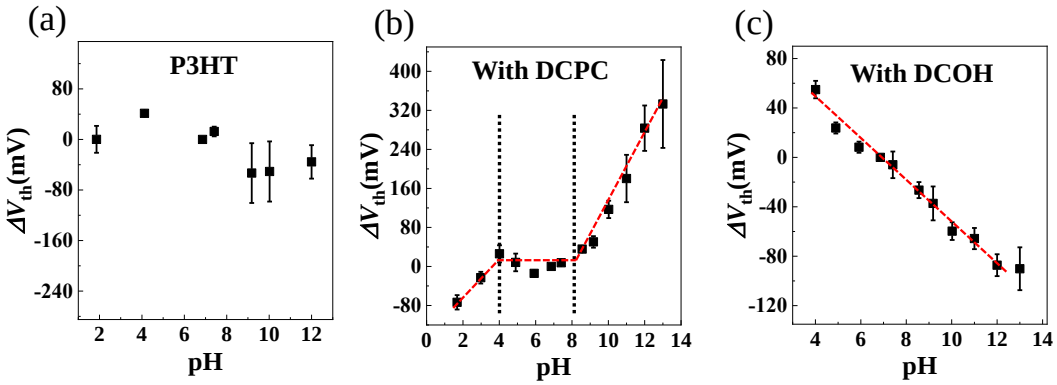
(a)
P3HT
ΔV_{th}(mV)
pH
(b)
With DCPC
ΔV_{th}(mV)
pH
(c)
With DCOH
ΔV_{th}(mV)
pH

Fig. 3.

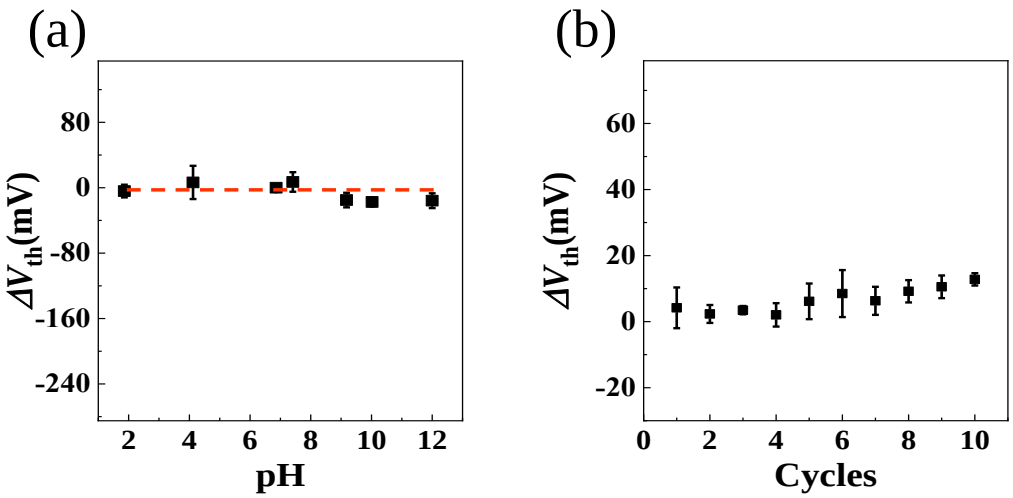
(a)
80
0
-80
-160
-240
ΔV_{th}(mV)
2
4
6
8
10
12
pH
(b)
60
40
20
0
-20
ΔV_{th}(mV)
0
2
4
6
8
10
Cycles

Fig. 4.